Characteristics of Vulnerable Occupants Predicted by Rib Structural Properties

Amanda M. Agnew, Matthew Wascher, Akshara Sreedhar, John H. Bolte IV, Jason Stammen, Kevin Moorhouse, Yun-Seok Kang

Abstract Recent advances in safety systems have reduced injuries sustained in motor vehicle crashes. However, unlike other body regions, rib fractures remain a common and serious injury in these events. The goal of this study was to assess the ability of basic individual demographic information to predict thoracic vulnerability. A normative sample of 317 experimentally-tested mid-level human ribs formed the foundation of this study, and the resulting structural properties of percent displacement, peak force, and total energy allowed for rib vulnerability levels to be defined for each property. Thresholds for these levels may be useful for alterations and assessment of rib FE models and improvement of thoracic scaling techniques. Additional results suggest that age, sex, stature, and weight may be utilized with caution for predicting those ribs that are *least* and *most* vulnerable, but are not useful for distinguishing those in between. Individuals more likely to have vulnerable ribs include those that are older with smaller body size, particularly females, but this is not always the case. Further investigation is necessary in order to identify more appropriate predictors for occupant vulnerability.

Keywords Fracture risk, injury, motor vehicle crash (MVC), thorax, vulnerability

I. INTRODUCTION

Despite vast improvements to recent injury mitigation systems in vehicles, thoracic skeletal injuries, i.e., rib fractures, are more likely to occur than injuries to any other body region in the event of a motor vehicle crash (MVC) [1]. Increasing age has been linked to frequency and severity of these thoracic injuries, and females tend to be at higher risk than males for rib fracture [2-3]. Furthermore, the occurrence of rib fractures from any cause leads to more serious outcomes for the elderly [4]. These data are very valuable as they are entirely based on real-world occurrences. However, these retrospective approaches can be difficult to interpret because all of the exact conditions and mechanisms of injury must be presumed or could be inaccurately reconstructed.

Therefore, quantification of the relationship between age, sex, and body size of occupants, and their likelihood of experiencing rib fracture, if all other aspects of an MVC were to be precisely equal, remains unknown because this would require a large experimental dataset in order to control all external variables. Agnew and colleagues [5] published such a dataset and reported relationships between human rib structural properties and demographics. This approach is useful for understanding variance in rib response that can be explained by individual characteristics, but quantifying the effectiveness of using demographics to predict risk for rib fracture, or vulnerability to injury, requires a slightly different approach.

Current injury assessment tools such as Human Body Models (HBMs) and Anthropomorphic Test Devices (ATDs) are generally less effective at representing demographics that vary from the average male, since most development in the past was focused on that demographic. Recent work [6] has highlighted the need for exploring more vulnerable populations in order to improve safety tools and establish more precise injury thresholds, but the biomechanical data to thoroughly do so are still lagging.

The objective of this study was to identify individual occupant characteristics that correspond to various levels of vulnerability to rib fractures based on experimental testing results. This was accomplished by first binning experimental rib data into five *vulnerability levels* based on percentiles of structural properties (displacement, force, energy), conducting an array of statistical tests to identify how the demographic factors (age, sex, stature, weight) varied with vulnerability level, and then constructing a proportional odds logistic regression model to predict vulnerability for a given individual.

AM Agnew (+1-614-366-2005; amanda.agnew@osumc.edu) is an Associate Professor, Y-S Kang an Assistant Professor, JH Bolte a Professor, and A Sreedhar an MS student at The Ohio State University (OSU) in the Injury Biomechanics Research Center (OH, USA). M. Wascher is with the Dept. of Statistics at OSU, OH, USA. J Stammen and K Moorhouse are affiliated with the National Highway Traffic Safety Administration, Vehicle Research and Test Center (NHTSA/VRTC) in East Liberty, OH, USA.

II. METHODS

Sample

Three hundred seventeen (n=317) mid-level (3-8) ribs representing various individual demographics were included in this sample. Male ribs comprised 230 of the ribs, while female ribs comprised 87. Despite the large number of male compared to female ribs, the age distribution between the sexes was not significantly different (two sample t-test, p=0.6), signifying that sex-specific comparisons were not biased by age. Ages ranged from six to 108 years (mean 52.6 ± 23.4 years). Individuals stature and weight at the time-of-death ranged from 117 to 199 cm (mean 172.7 ± 11.3 cm) and 19 to 152 kg (mean 71.9 ± 19.3 kg), respectively. Age, sex, stature, and weight are the individual characteristics of interest in this study, and their distributions in the rib sample can be found in Fig. A1.

Experimental Testing

Excised whole human ribs were experimentally tested in a custom pendulum fixture representing a simplified frontal thoracic blunt impact. The fixture included a 6-axis load cell (CRABI neck load cell, IF-954, Humanetics, Plymouth, MI, USA) behind the stationary plate, and a linear string potentiometer (Rayelco P-20A, AMETEK, Inc. Berwyn, PA, USA) attached to the moving plate to measure force and displacement, respectively, in the primary loading direction (-X) as shown in Fig. 1. Rib ends were potted in Bondo® Body Filler (Bondo Corporation, Atlanta, GA, USA) allowing for a single-plane orientation and therefore translation of the sternal rib end towards the vertebral end during this 2D bending event. Dynamic impacts were conducted at 2 m/s (~0.5 strain/s) with the goal of loading ribs to failure. Additional details of rib preparation can be found in [5].

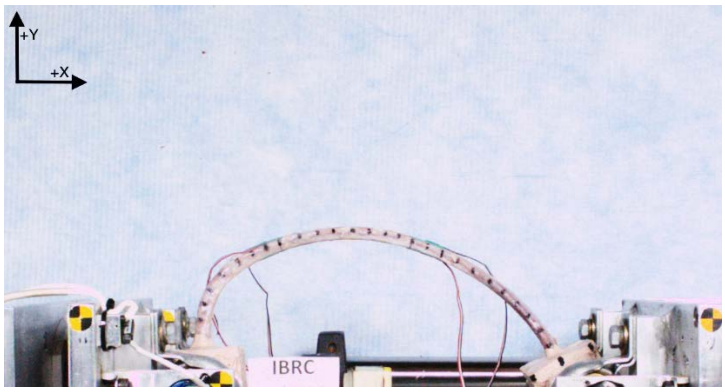

Fig. 1. Experimental test set-up with rib in fixture pre-impact (adapted from [7])

Data Analysis

Force and displacement data were filtered using a CFC180 filter [5]. Utilizing the force-displacement (F-D) curve from each impact, peak displacement and peak force (F_{peak}) were defined as the maximum displacement and force, respectively, in the primary loading direction prior to fracture. Peak displacement was then normalized by the original mechanical span of each rib to calculate a percent displacement (δ), referred to simply as *displacement* throughout the manuscript. Total energy (U_{tot}) was calculated as the area beneath the F-D curve from time zero to time of failure.

The structural properties of percent displacement (δ), peak force (F_{peak}), and total energy (U_{tot}) were each divided into five levels of vulnerability per rib based on the accumulation of 20th percentiles: 1 was defined as most vulnerable and 5 as least vulnerable. It was assumed that lower structural property values were equivalent to greater vulnerability. Differences in vulnerability levels were first explored relative to age, stature, and weight using Analysis of Variance (ANOVA) with Tukey's post-hoc tests to identify sources of potential differences between each level. Once differences were identified, the ability to predict vulnerability based on individual demographics was assessed. For each structural property, a proportional odds logistic regression model in R

statistical computing software (v. 3.6.3) was fit using the polr function from the Modern Applied Statistics with S (MASS) package to classify individual ribs into vulnerability levels 1 through 5 using the demographic covariates. For the purposes of fitting these models, vulnerability level was considered an ordinal variable and predictors from the available covariates were selected using the Bayesian Information Criteria (BIC) model selection technique for each model. This approach assumes that for each level j = 1, . . . 5, the log odds ratio $log(\frac{P(Y \leq j)}{P(Y > j)})$ is a linear function of the covariates. This linear function is allowed a different intercept for each j, but assumed to have the same slope for all j. The coefficient β_i associated with a predictor can be interpreted as the change in the log odds ratio $log(\frac{P(Y \leq j)}{P(Y > j)})$ when that predictor is increased by 1 unit, and this quantity is the same for all j = 1, . . . 5. It is then possible to use the predicted log odds ratios for a given set of covariates to compute the predicted probability that an individual with those covariates falls into each of the 5 vulnerability levels. The predicted vulnerability level for a rib from an individual with a given set of characteristics was then taken to be the vulnerability level that the model assigns the highest probability of that individual's rib falling into.

To test whether the estimated coefficients in the proportional odds logistic regression were different from 0, the following approach was utilized: for each predictor, the Central Limit Theorem implies that the estimated coefficient divided by its standard error is asymptotically normally distributed with mean 0 and standard deviation 1. Since the sample is sufficiently large, an approximate z-test was applied to obtain p-values for the test of the hypothesis: $H0: \beta i = 0$ versus $H1: \beta i \neq 0$

for each of the predictors. Additionally, for each vulnerability level, 1 through 5, an individual was identified in the sample whom the model assigned the highest probability of falling into that particular vulnerability level. These individuals, along with their characteristics, are presented as informal exemplars of each level.

A subsample was subsequently identified with the goal of separating out only two extremely distinct groups *vulnerable* and *invulnerable* based on the combination of all structural properties. The vulnerable category was defined by those ribs that previously scored a level 1 vulnerability for at least two of the structural properties and a level 2 vulnerability in the third. The invulnerable category was similarly defined by those ribs that previously scored a level 5 vulnerability for at least two of the structural properties and a level 4 vulnerability in the third. Coincidently, this resulted in both groups including 49 ribs each. Differences in age, stature, and weight between vulnerable and invulnerable ribs were assessed using ANOVA, and differences in sex were assessed using a Chi-squared association test. An alpha (α) value of 0.005 was used to determine statistical significance.

III. RESULTS

Descriptive statistics for each level of vulnerability (1-5) for each structural property independently are presented in Table I. These include the mean and one standard deviation as well as the range (minimum to maximum) for each property and associated time at fracture ($Time_{fx}$) for each vulnerability level. Because there was a strong positive linear relationship between percent displacement and time at fracture, it is possible to predict fracture timing from percent displacement (Linear Regression, adj. R^2 = 83.4%, p<0.0001, $Time_{fx} = 9.019 + 0.9867\delta$) to alter rib FE models if desired.

ANOVA was utilized to explore preliminary differences between the five vulnerability levels for each continuous variable, i.e., age, stature, and weight, by individual structural properties. Results of this exploration can be found in Table II and Fig. A2. Vulnerability levels were able to be delineated by age for displacement (p<0.0001, Fig. 2a), peak force (p=0.001), and total energy (p<0.0001). Common to all three, post-hoc analyses identified the least vulnerable level (5) as significantly different than the other levels. Vulnerability levels were successfully delineated by stature (Fig. 2b) and weight for peak force (p<0.0001), with level 1 identified as significantly different than the other levels. Similarly, stature and weight were significantly different between the most vulnerable (1) and least vulnerable (4-5) levels for total energy (p=0.004, p<0.0001, respectively).

TABLE I

DESCRIPTIVE STATISTICS OF RIB PROPERTIES FOR FIVE VULNERABILITY LEVELS*

	1 Mean(SD) Min-Max	2 Mean(SD) Min-Max	3 Mean(SD) Min-Max	4 Mean(SD) Min-Max	5 Mean(SD) Min-Max
			Displacement		
δ (%)	12.7(1.5) 0-14.7	17.1(1.5) 14.8-19.5	21.1(1.1) 19.6-23.3	26.7(2.2) 23.4-30.2	43.4(11.2) 30.3-68.5
$Time_{fx}$ (ms)	21.2(3.8) 11.3-26.8	25.6(4.5) 16.8-34.3	30.9(4.9) 20.8-41.6	36.3(5.6) 21.4-46.8	50.6(14.5) 29.0-101.0
			Peak Force		
F_{peak} *(N)*	49.5(12.4) 0-65.8	77.0(5.3) 65.9-85.5	98.6(6.8) 85.6-111.0	125.5(9.1) 111.1-140.6	176.2(33.3) 140.7-299.8
$Time_{fx}$ (ms)	27.8(7.4) 11.3-46.3	32.9(14.4) 12.8-81.9	31.3(11.9) 15.9-85.5	37.4(14.9) 14.7-101.0	35.0(11.9) 13.8-85.6
			Total Energy		
U_{tot} *(N*mm)*	993(314) 0-1416	1733(221) 1417-2166	2626(307) 2167-3228	4166(554) 3229-5299	7922(2609) 5300-16154
$Time_{fx}$ (ms)	22.8(4.6) 11.3-32.9	26.6(6.1) 14.6-39.4	31.5(6.6) 15.9-46.3	34.3(8.5) 13.8-55.2	49.4(15.0) 24.8-101.0

*1=most vulnerable, 5=least vulnerable. SD= one standard deviation. $Time_{fx}$= time of fracture

TABLE II

ANOVA RESULTS FOR VULNERABILITY LEVELS

	Displacement		**Peak Force**		**Total Energy**	
	R-sq (adj) %	p-value	R-sq (adj) %	p-value	R-sq (adj) %	p-value
Age	28.4	<0.0001	4.5	0.001	18.8	<0.0001
Differences	5<(1=2=3=4)		(4=5)<1		5<(1=2=3=4)	
Stature	0.3	0.30	12.3	<0.0001	3.7	0.004
Differences	None		1<(2=3=4=5)		1<(4=5)	
Weight	0.2	0.35	14.5	<0.0001	6.5	<0.0001
Differences	None		1<(3=4=5)		1<(4=5)	

Differences are results of Tukey post-hoc tests between vulnerability levels

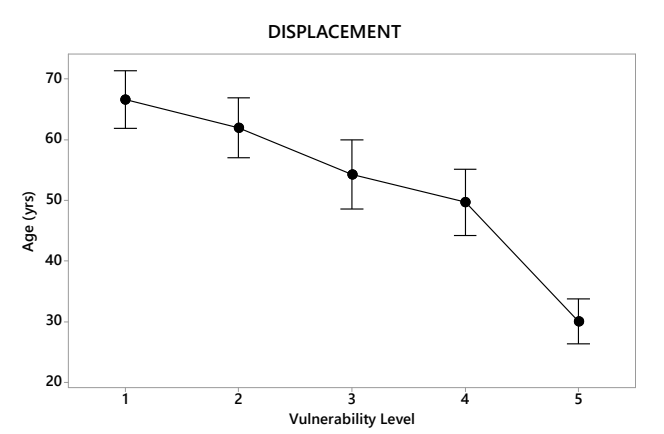

Fig. 2a. Interval plot (mean and 95% CI) comparing age between vulnerability levels for displacement. Level 5 is significantly different (p<0.0001).

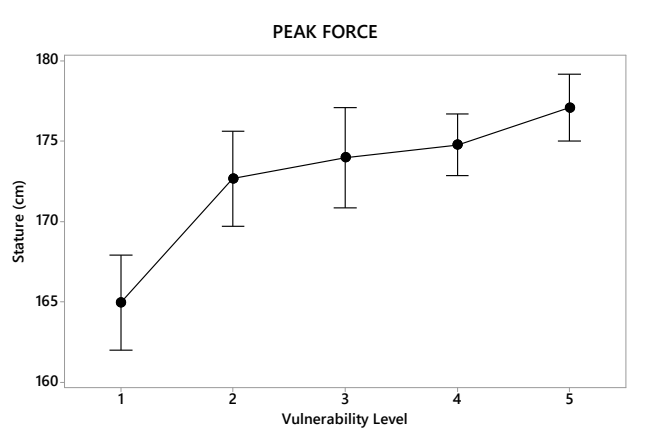

Fig. 2b. Interval plot (mean and 95% CI) comparing stature between vulnerability levels for peak force. Level 1 is significantly different (p<0.0001).

Since differences between vulnerability levels were successfully established using a simple ANOVA, the next step was to explore the capacity to classify individuals accurately into vulnerability levels utilizing a predictive model. In order to quantify the ability to use age, sex, stature, and weight to predict vulnerability, a proportional odds logistic regression was utilized. Figs. A3-A5 provide visual representation of this approach to exploring initial relationships between predictor combinations by vulnerability levels.

Figs. 3-5 and Table III display the results of classifying individuals with the proportional odds logistic regression models for each of the three structural properties. For displacement, the proportional odds logistic regression model incorporated age, sex, and stature, with only age and sex making significant contributions to the model. The peak force model incorporated age, sex, weight, stature, and the interaction of age*sex. For this model, sex was not a significant contributor on its own, but was when accounting for interaction with age. For total energy, the model included age, weight, stature, sex, and the interaction of age*sex. Age and sex significantly contributed to all three models in some way. Stature did not contribute predictive value to any of the models, but weight did for peak force and total energy. Details for each individual model are in Table III.

In general, the proportional odds logistic regression models were fairly successful in predicting vulnerability levels 1 and 5, and, on average, assigned higher predicted vulnerability to ribs from actual higher levels. However, all models were less successful at predicting and differentiating among the middle levels, 2-4. In particular, the displacement model predicted levels 1 and 5 well (Fig. 3), and the peak force model predicted level 1 well (Fig. 4). The total energy model was less successful than the others at prediction of levels 1 and 5 (Fig. 5).

Additionally, the model was queried to select an individual rib as the best representation of each vulnerability level for each property, chosen based on having the highest probability of falling within that level. This is reported as demographics for each selected rib as well as a comparison between the predicted vulnerability and the actual vulnerability (Table IV). For all three properties, the predicted and actual vulnerabilities matched for level 1 and level 5, indicating these models utilizing the predictors previously discussed can successfully identify those on the extremes of vulnerability. However, the model was rarely able to accurately predict levels 2-4. In only two cases out of nine possible, did the predicted and actual vulnerabilities match in the middle levels.

TABLE III

PROPORTIONAL ODDS LOGISTIC REGRESSION MODELS

	Chosen Parameters:	Age	Male†	Stature		
***δ* model**	β_i *Coefficient*	-0.0500	-1.1213	0.0240		
	Std. Error	0.0052	0.2820	0.0105		
	P-value	**<0.0001**	**<0.0001**	0.023		
	Chosen Parameters:	Age	Male†	Weight	Stature	Age:Male†
***F_{peak}* model**	β_i *Coefficient*	-0.0559	-1.1522	0.0279	0.0163	0.0437
	Std. Error	0.0105	0.6257	0.0068	0.0125	0.0119
	P-value	**<0.0001**	0.065	**<0.0001**	0.191	**0.0002**
	Chosen Parameters:	Age	Weight	Stature	Male†	Age:Male†
***U_{tot}* model**	β_i *Coefficient*	-0.0742	0.0224	0.0221	-2.1693	0.0428
	Std. Error	0.0101	0.0068	0.0124	0.6166	0.0115
	P-value	**<0.0001**	**0.001**	0.075	**0.0004**	**0.0002**

†Coefficients can be applied as listed if reference is male. Significant p-values are **bolded**.

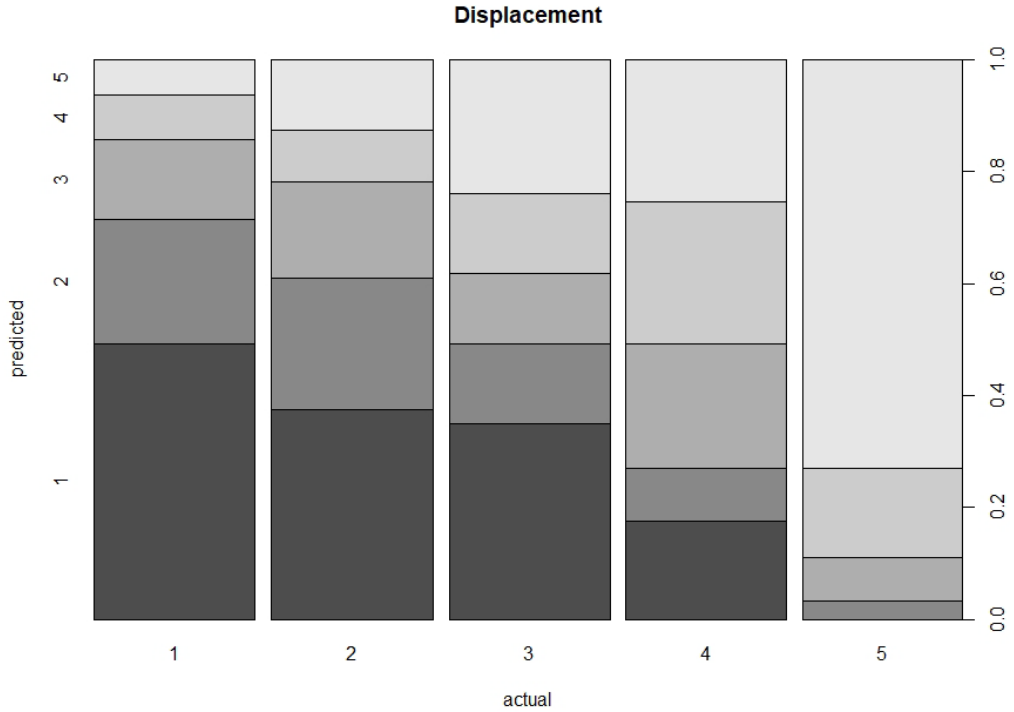

Fig. 3. Comparisons of actual versus predicted classifications of vulnerability (levels 1-5) for displacement. The shaded boxes on the vertical axes indicate what proportion of individuals in each vulnerability level (actual) were assigned to each level (predicted) by the proportional odds logistic regression model. Level 1 is the darkest, level 5 the lightest.

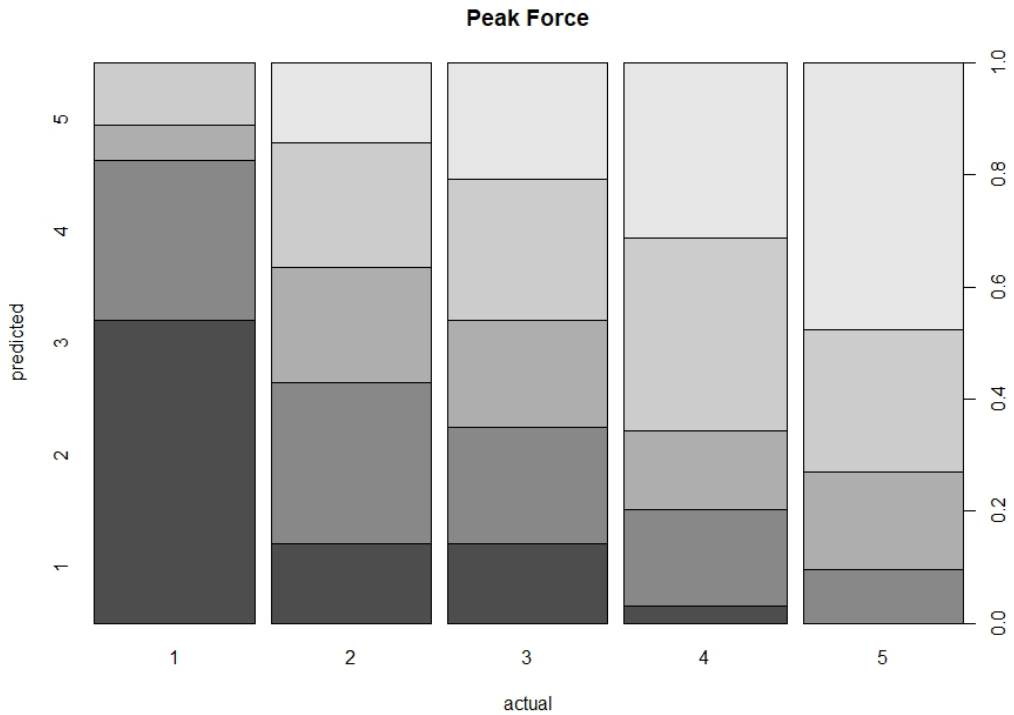

Fig. 4. Comparisons of actual versus predicted classifications of vulnerability (levels 1-5) for peak force.The shaded boxes on the vertical axes indicate what proportion of individuals in each vulnerability level (actual) were assigned to each level (predicted) by the proportional odds logistic regression model. Level 1 is the darkest, level 5 the lightest.

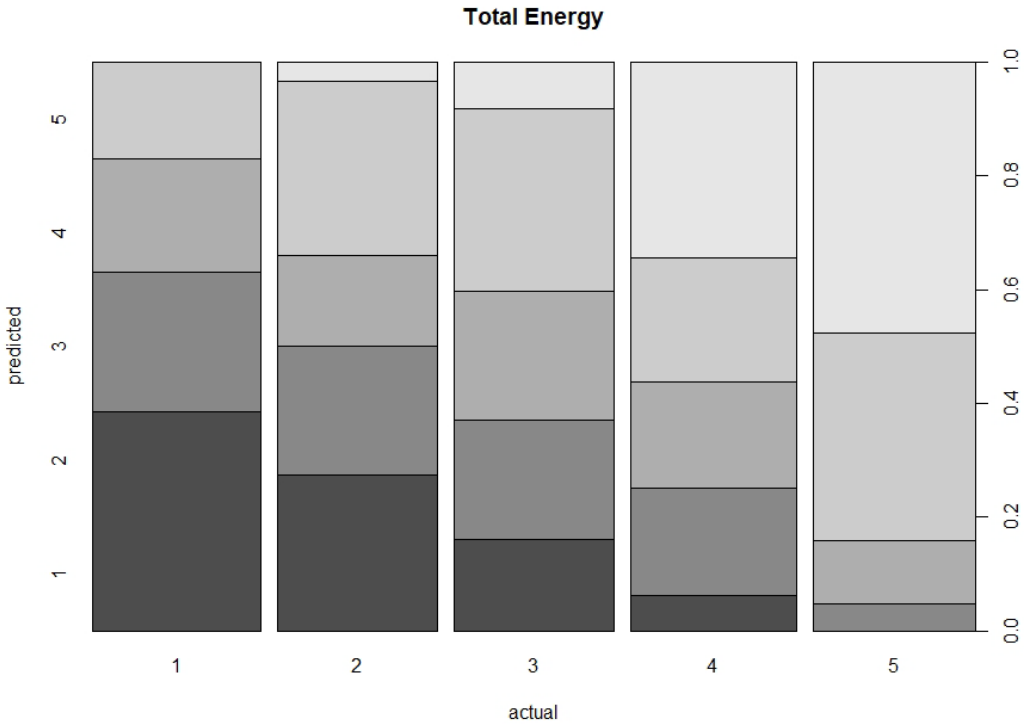

Fig. 5. Comparisons of actual versus predicted classifications of vulnerability (levels 1-5) for total energy. The shaded boxes on the vertical axes indicate what proportion of individuals in each vulnerability level (actual) were assigned to each level (predicted) by the proportional odds logistic regression model. Level 1 is the darkest, level 5 the lightest.

TABLE IV
REPRESENTATIVE INDIVIDUALS FOR EACH VULNERABILITY LEVEL

	Predicted Vulnerability	Age (yrs)	Sex	Stature (cm)	Weight (kg)	Structural Property	Actual Vulnerability	Match
δ (%) model	1	97	M	149.9	78.9	14.6	1	YES
	2	75	M	183.0	84.8	21.6	3	NO
	3	52	M	181.0	83.0	11.5	1	NO
	4	29	M	180.3	90.0	39.0	5	NO
	5	11	F	160.2	50.5	51.38	5	YES
F_{peak} (N) model	1	92	F	142.2	32.2	40.9	1	YES
	2	22	M	139.7	29.5	76.7	3	NO
	3	71	M	180.0	68.0	105.2	3	YES
	4	17	F	165	76.0	145.8	5	NO
	5	24	F	165.1	152.0	206.7	5	YES
U_{tot} (N*mm) model	1	92	F	142.2	32.2	926	1	YES
	2	86	M	185.4	56.2	1328	1	NO
	3	62	M	172.7	84.4	551	1	NO
	4	44	M	182.9	99.8	4310	4	YES
	5	18	F	167.6	136.0	6455	5	YES

When all structural properties were combined to create only two extreme subsamples of *vulnerable* or *invulnerable*, all differences between these two groups for age, stature, weight, and sex were highly significant as shown in Table V ($p<0.001$). This analysis was conducted in order to identify the features of occupants *most* at risk for rib fractures. Those individuals with vulnerable ribs were, on average, older and smaller in both stature and weight. Expected versus observed frequencies of sex in each category were also significantly different. However, this was likely driven by an imbalance between numbers of males and females in the

invulnerable category (M>F). While it was expected that more females would be represented than males in the vulnerable category, this was not the case, as both sexes were essentially equally represented. In other words, while males are more likely than females to have invulnerable ribs, they are equally likely to have vulnerable ribs as females.

TABLE V
DEMOGRAPHIC COMPARISONS BETWEEN VULNERABLE AND INVULNERABLE GROUPS

	Vulnerable (n=49)		**Invulnerable (n=49)**		**p-value**
	Mean(SD)	95% CI	Mean(SD)	95% CI	
Age (yrs)	68.8(20.5)	63.4,74.3	35.6(17.7)	30.2 41.1	<0.0001
Stature (cm)	168.5(11.7)	165.7,171.3	177.1(7.7)	174.3,179.9	<0.0001
Weight (kg)	63.7(17.7)	58.7,68.7	81.0(17.5)	76.0,86.0	<0.0001
Sex†	M(26), F(23)		M(41), F(8)		<0.001

ANOVA was used for all comparisons except for sex. †Actual frequencies for sexes in each category are reported here and were used in a Chi-Square Test for association.

IV. DISCUSSION

The findings presented in the current study are consistent with real world data that identifies elderly, small individuals as being the most vulnerable vehicle occupants [8]. However, these results are more impactful than simply reiterating existing observations. Because of the vast size of the sample in the larger rib study this is a part of, these data can be interpreted as a normative dataset, allowing for the opportunity to provide thresholds and targets for displacement, force, and energy relative to time at fracture in order for researchers to assign levels of vulnerability to ribs in FE models.

Based on the simple assessment of vulnerability level differences via ANOVA, a few broad trends emerged. First, contrary to the common approach, i.e., advanced age is often used as an explanation of increased fragility, age appears to be most useful in identifying those ribs which are *least* vulnerable, i.e. in level 5, while differences in age between the other vulnerability levels are more subtle. In other words, it is possible to more confidently conclude that younger individuals have less vulnerable ribs than to say that older individuals have more vulnerable ribs. This is most apparent for vulnerability based on structural properties of displacement and total energy. Age is less effective in identifying the least vulnerable using peak force, but this simple analysis is capable of delineating vulnerability levels 4 and 5 together from the more vulnerable levels. Next, stature and weight follow similar patterns to each other and these trends allow for identification of those ribs which are most vulnerable (the opposite of what age told us). Those individuals that are short in stature and weigh less, i.e., small body size, have ribs which are most vulnerable, i.e., in level 1, for peak force and total energy (no relationships exist with displacement). Differences between the other vulnerability levels are not as clear for body size parameters. This may suggest that some component of the increased injury risk seen for very small or large occupants may not necessarily be dictated by intrinsic variability in the bone itself, but rather to external influences (e.g., mass effects on kinematics, belt interaction and fit) [9].

Sex was a significant contributor, either alone or when interacting with age, for all regression models. This further strengthens the evidence that females are not just simply smaller versions of males [10], and supports future work to evaluate fracture risk and vulnerability independently in females, in parallel with males. Injury thresholds have not often been experimentally derived separately for the sexes, and quantification of these differences may have large effects on scaling and interpretation of data in HBMs and ATDs.

Utilizing proportional odds logistic regression models, it was possible to fairly successfully predict the least and the most vulnerable individuals, but this was not the case for the majority of individuals that fell between these extremes. None of the models predicted a vulnerability level 1 for a rib that was actually a 5. Similarly, the peak force (Fig. 4) and total energy (Fig. 5) models never predicted a level 5 when a rib was actually a 1, but this type of error did occur in the displacement model (Fig. 3). When exploring the model's selection of the most

representative individual for each vulnerability level (Table IV), the greatest discrepancy seemed to exist for not only the middle levels, but specifically for level 3. For both displacement and energy models, selected individuals to best represent level 3 were actually a level 1. This direction of prediction error could have major implications. However, in most other cases where vulnerability level was not matched between actual and predicted, the model predicted the representative individual to be more vulnerable than they actually were (e.g., the force model predicted a level 4 but the individual was actually a level 5). In terms of developing mitigation strategies for occupant injury, it is more desirable to overpredict vulnerability than to underpredict it. In other words, safety technology should target protection of the most vulnerable occupants, assuming the others will also be protected. Further exploration is necessary to minimize and direct such errors as well as differentiate the middle vulnerability levels for future applications.

Multiple researchers have attempted to predict rib structural properties utilizing demographic information [5][7][11][12], but none have attempted to predict individual characteristics based on a normative dataset defining vulnerability as was done here. These previous studies were variably successful in identifying relationships between age, sex, and body size with rib properties, but concede that most variability in rib response to loading remains unexplained, and that further research is necessary. Even when taking the fresh approach presented here, the highest proportion for a successful prediction was about 75% (vulnerability level 5 for the displacement model), while the other most successful predictions only reached approximately 50-60% (generally levels 1 and 5 for all models). This suggests it is important to explore additional new variables in future work to predict differential rib fracture risk and biomechanical response to define occupant vulnerability.

There were several limitations to this study. The rib dataset included considerably more males than females, and non-normal stature and weight data. Although all approaches utilized here were robust against these data inconsistencies, they could possibly bias the results. The experimental data were acquired from a simplified 2D bending scenario on excised ribs. The boundary conditions of the test were deliberately oversimplified in order to ensure repeatability in loading, but did not consider rib angle or an offset for costal cartilage. Additionally, isolated ribs will never be loaded in real events, as each rib is, of course, only a part of the larger articulated thorax. It is unknown how these results may translate to full thoracic response and injury risk. In spite of the lack of a normative dataset for full body experimental testing, this rib dataset, the largest known collection of biomechanical data on various individuals, can fill an important gap in knowledge for the vehicle safety community.

V. CONCLUSIONS

Until new technologies arise that allow for direct measurement of rib bone quality and associated fracture risk, researchers can utilize these results to identify general rib vulnerability for an occupant based on basic demographic information. This should be attempted with caution until it is possible to increase the proportional odds of classifying individuals with greater confidence. Furthermore, the thresholds for vulnerability levels based on the normative dataset presented here can be utilized in rib FE models and HBMs to explore vulnerable occupant rib response. Age and sex varied considerably between vulnerability levels, while stature and weight showed more variable results, but still some value in identifying rib vulnerability: relatively young individuals and males tended to have less vulnerable ribs, while those with smaller body size tended to have more vulnerable ribs. This approach was most successful at predicting the particularly vulnerable or particularly invulnerable ribs based on demographics.

VI. ACKNOWLEDGEMENT

We are greatly indebted to the anatomical donors that have made this research possible. The views expressed within are solely those of the authors and do not represent the opinions of any sponsor. Also, thanks to all students and staff of the Injury Biomechanics Research Center at The Ohio State University, especially Angela Harden, Randee Hunter, Arri Willis, Rakshit Ramachandra, Aubrie Sanchez, and Michelle Murach.

VII. REFERENCES

[1] Forman J, Poplin G, et al. Automobile injury trends in the contemporary fleet: Belted occupants in frontal collisions. *Traffic Injury Prevention*, 2019, 20(6):607-612.

[2] NHTSA. Technical Report: Injury vulnerability and effectiveness of occupant protection technologies for older occupants and women. *National Highway Traffic Safety Administration*, 2013, DOT HS 811 766.

[3] Wisch M, Lerner M, Vukovic E, Hynd D, Fiorentino A, Fornells A. Injury patterns of older car occupants, older pedestrians or cyclists in road traffic crashes with passenger cars in Europe - Results from SENIORS. *International Research Council on Biomechanics of Injury (IRCOBI)*, Antwerp, Belgium, 2017, IRC-17-17:63-78.

[4] Bergeron E, Andre L, et al. Elderly trauma patients with rib fractures are at a greater risk of death and pneumonia. *Journal of Trauma*, 2003, 54:478-485.

[5] Agnew AM, Murach MM, et al. Sources of variability in structural bending response of pediatric and adult human ribs in dynamic frontal impacts. *Stapp Car Crash Journal*, 2018, 62:119-192.

[6] Shurtz B, Agnew AM, Kang Y-S, Bolte JH. Application of scaled deflection injury criteria to two small, fragile females in side impact motor vehicle crashes. *Proceedings of World Congress of Biomechanics, SAE International*, 2018, 2018-01-0542.

[7] Agnew AM, Murach MM, Misicka E, Moorhouse K, Bolte JH, Kang Y-S. The effect of body size on adult human rib structural properties. *International Research Council on Biomechanics of Injury (IRCOBI)*, 2017, IRC-17-105:728-736.

[8] Ramachandra R, Kashikar T, Bolte JH. Injury patterns of elderly occupants involved in side crashes. *Proceedings of International Research Council on Biomechanics of Injury (IRCOBI) Conference*, Antwerp, Belgium, 2017, IRC-17-21:113-115.

[9] Kent, R., Forman, J., & Bostrom, O. (2010). Is there really a "cushion effect"?: A biomechanical investigation of crash injury mechanisms in the obese. Obesity, 18, 749-753.

[10] Schlecht S, Bigelow E, Jepsen K. How does bone strength compare across sex, site, and ethnicity? *Clinical Orthopaedics and Related Research*, 2015, 473(8):2540-2547.

[11] Agnew AM, Moorhouse K, et al. The response of pediatric ribs to quasi-static loading: Mechanical properties and microstructure. *Annals of Biomedical Engineering*, 2013, 41(12):2501-2514.

[12] Kalra A, Saif T, et al. Characterization of human rib biomechanical response due to three-point bending. *Stapp Car Crash Journal*, 2015, 59:113-130.

VIII. APPENDIX

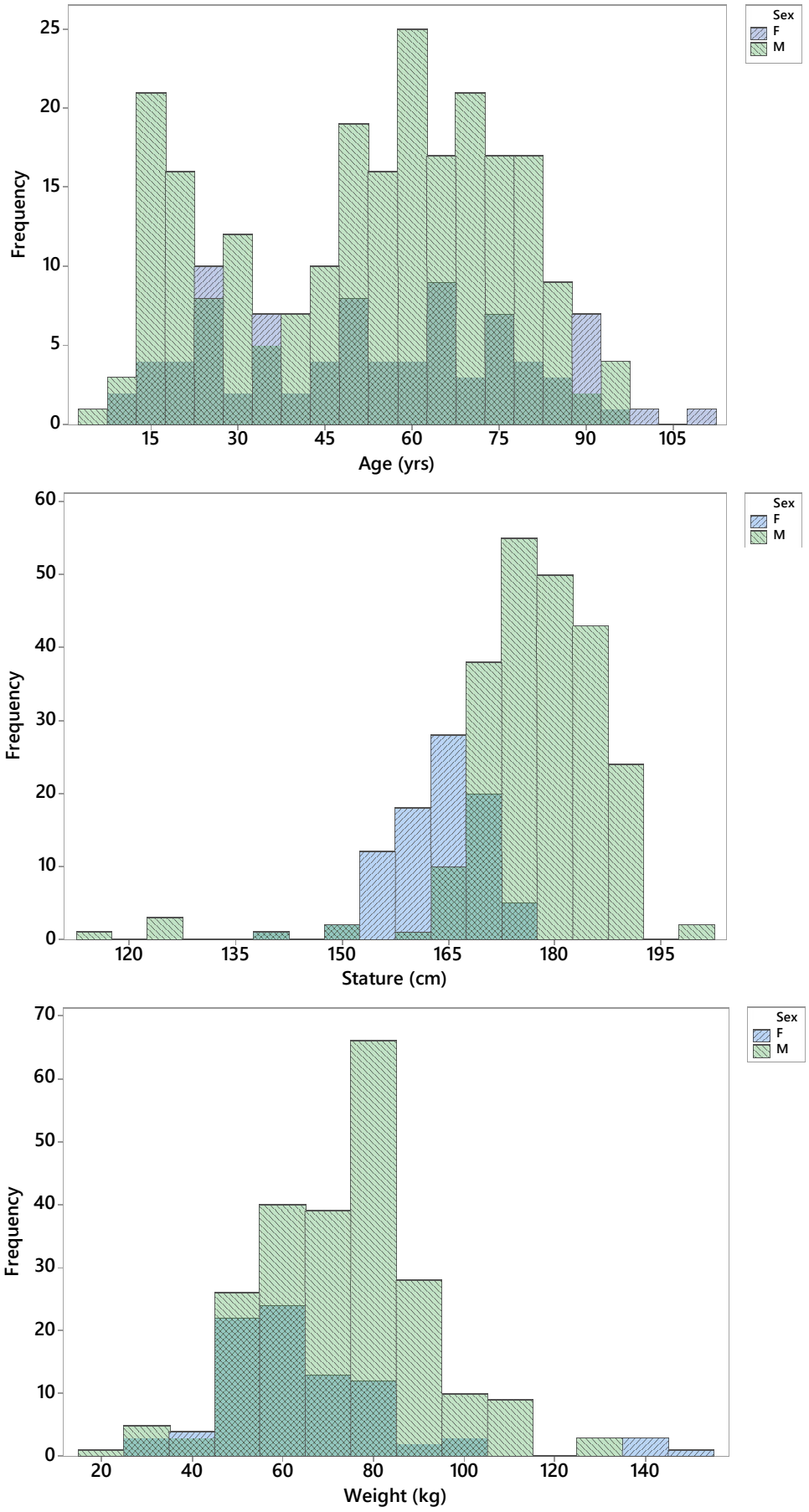

Fig. A1. Histograms of age (top), stature (middle), and weight (bottom) by sex showing distributions of ribs

TABLE AI

DESCRIPTIVE STATISTICS FOR DEMOGRAPHICS BY STRUCTURAL PROPERTIES AND VULNERABILITY LEVELS*

	1 Mean(SD) 95% CI	**2** Mean(SD) 95% CI	**3** Mean(SD) 95% CI	**4** Mean(SD) 95% CI	**5** Mean(SD) 95% CI
			Displacement		
Age (yrs)	66.6(18.9) 61.7,71.6	62.0(19.8) 57.1,66.8	54.3(22.8) 49.4,59.2	49.7(22.0) 44.8,54.6	30.1(14.7) 25.2,35.0
Stature (cm)	172.7(8.3) 169.9,175.5	173.8(11.5) 171.0,176.5	173.9(11.1) 171.1,176.7	173.1(13.8) 170.3,175.9	170.0(10.5) 167.3,172.8
Weight (kg)	73.5(16.6) 68.7,78.2	71.6(20.0) 66.9,76.4	67.9(16.4) 63.1,72.7	71.9(18.7) 67.2,76.6	74.7(23.6) 69.9,79.5
Sex†	M(50), F(13)	M(49), F(15)	M(50), F(13)	M(44), F(20)	M(37), F(26)
			Peak Force		
Age (yrs)	61.0(26.8) 55.4,66.7	54.2(24.1) 48.6,59.8	54.8(22.0) 49.1,60.5	46.1(21.8) 40.5,51.7	46.7(18.9) 41.1,52.4
Stature (cm)	165.0(11.8) 162.4,167.6	172.7(11.7) 170.1,175.3	174.0(12.4) 171.4,176.6	174.8(7.7) 172.2,177.4	177.1(8.2) 174.5,179.7
Weight (kg)	58.7(16.6) 54.2,63.1	69.5(17.6) 65.1,73.9	73.6(19.1) 69.1,78.0	76.9(17.0) 72.5,81.2	81.0(18.8) 76.5,85.4
Sex†	M(27), F(36)	M(44), F(20)	M(53), F(10)	M(53), F(11)	M(53), F(10)
			Total Energy		
Age (yrs)	65.5(22.2) 60.3,70.7	57.4(24.2) 52.1,62.7	55.5(21.6) 50.3,60.8	49.0(19.7) 43.8,54.2	35.1(17.8) 29.8,40.3
Stature (cm)	168.3(12.6) 165.6,171.0	173.2(8.8) 170.4,176.0	172.6(14.1) 169.8,175.3	173.9(10.3) 171.1,176.6	175.8(8.4) 173.0,178.5
Weight (kg)	64.3(19.2) 59.8,68.9	69.4(15.5) 64.7,74.0	70.3(18.1) 65.7,74.9	76.2(20.1) 71.6,80.8	79.4(19.9) 74.8,84.1
Sex†	M(39), F(26)	M(47), F(15)	M(48), F(15)	M(48), F(16)	M(48), F(15)

*1= vulnerable, 5=least vulnerable. †Sex is frequency of M (males) and F (females)

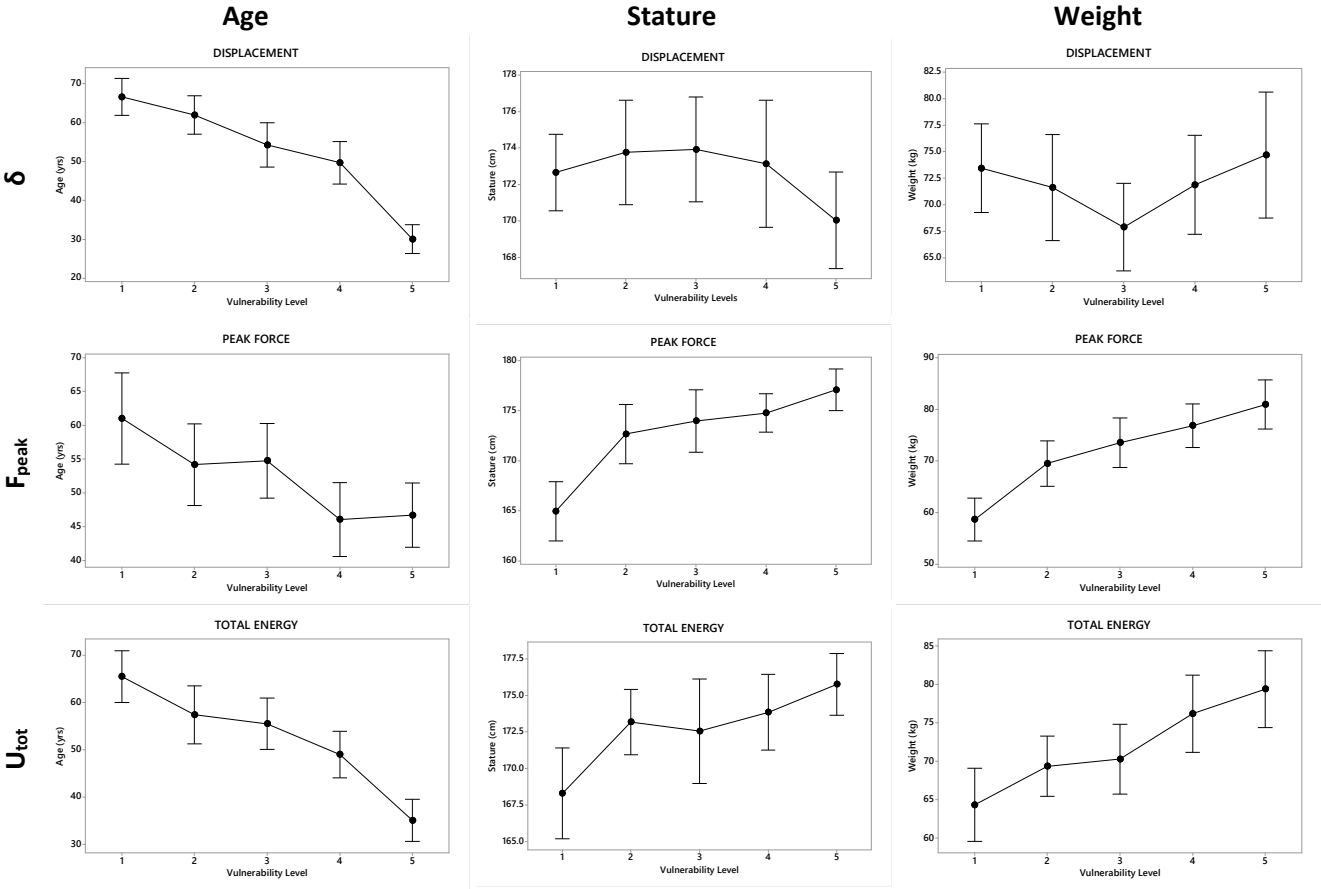

Fig. A2. Interval plots (mean and 95% CI) comparing all combinations of structural properties and demographics by vulnerability levels to accompany ANOVA results in Table II and AI

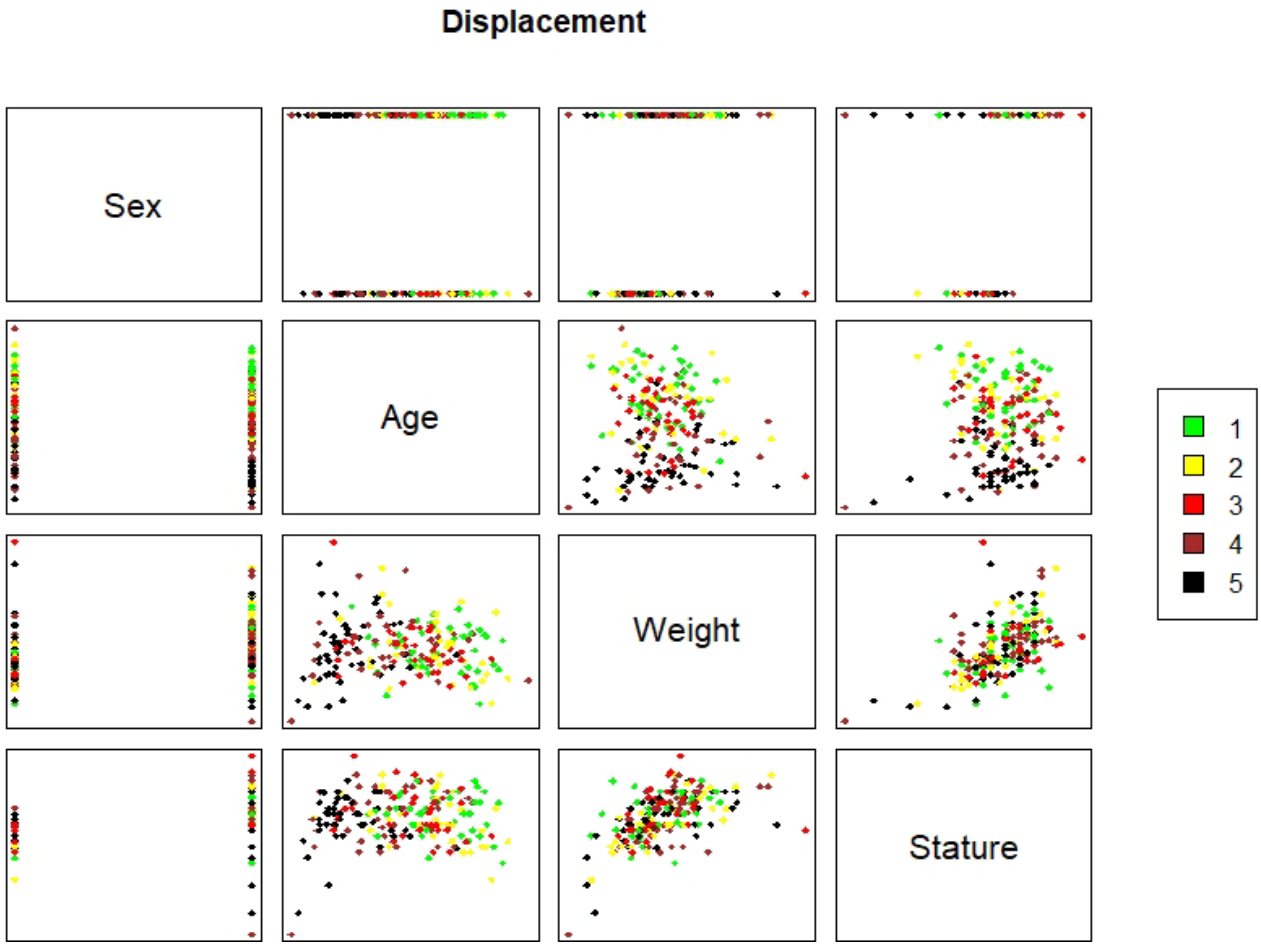

Fig. A3. Exploratory data analysis for all combinations of individual characteristics by vulnerability level (see legend) for displacement. Clustering of light datapoints (vulnerable) versus dark datapoints (less vulnerable) indicates which variables can best distinguish between vulnerability levels. Specific observations to note include: 1) for each sex, vulnerability is greater at older ages, but sex differences in vulnerability do not seem evident with trends of weight or stature, 2) clustering by age is apparent across all variables, and 3) no vulnerability clustering is apparent for interactions of weight and/or stature.

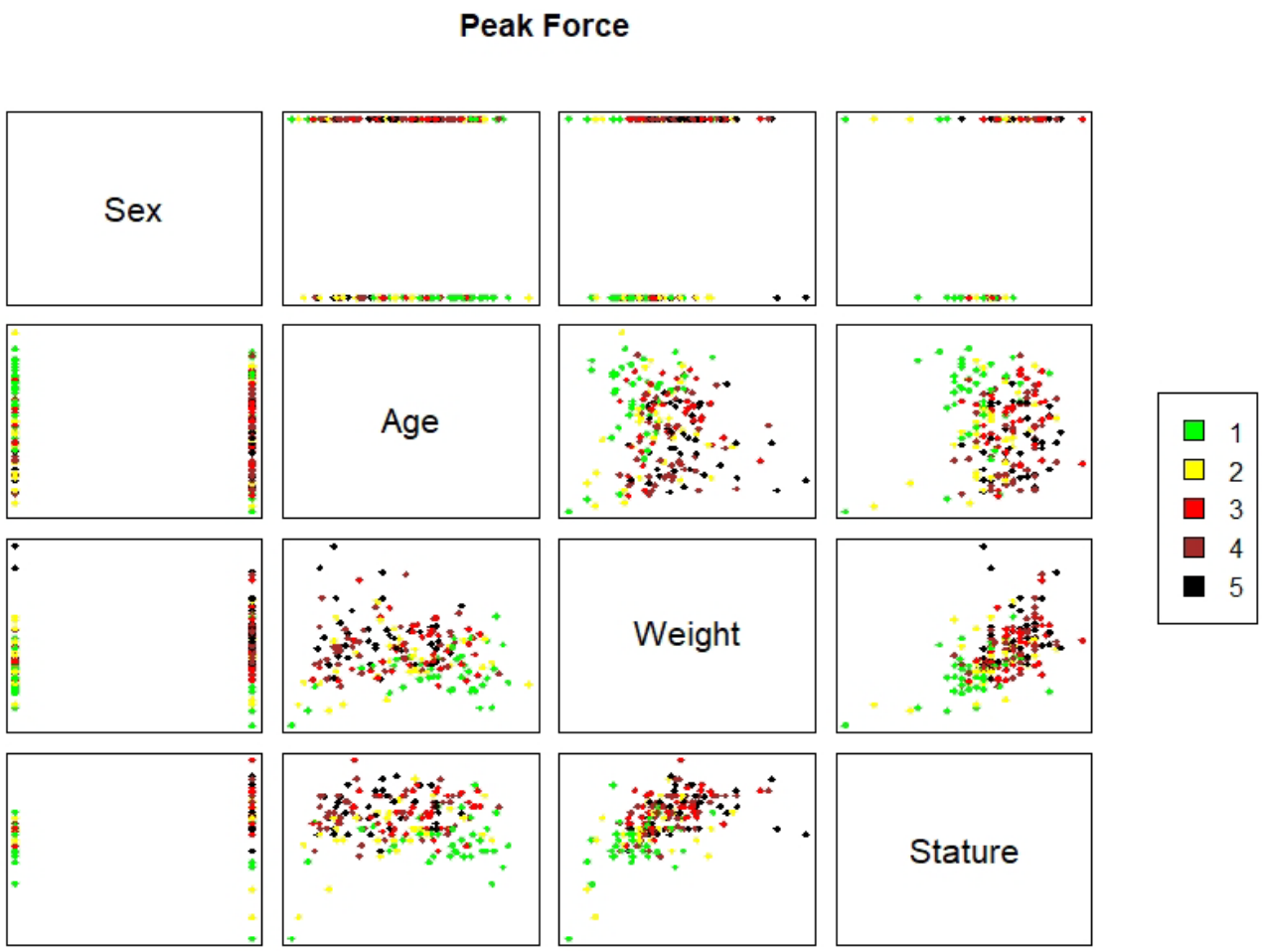

Fig. A4. Exploratory data analysis for all combinations of individual characteristics by vulnerability level (see legend) for peak force. Clustering of light datapoints (vulnerable) versus dark datapoints (less vulnerable) indicates which variables can best distinguish between vulnerability levels. Specific observations to note include: 1) vulnerability is greater at older ages, particularly for females, 2) clustering by age is not as apparent across variables, and 3) vulnerability clustering is apparent for interactions of weight and/or stature, especially for extreme vulnerability (level 1).

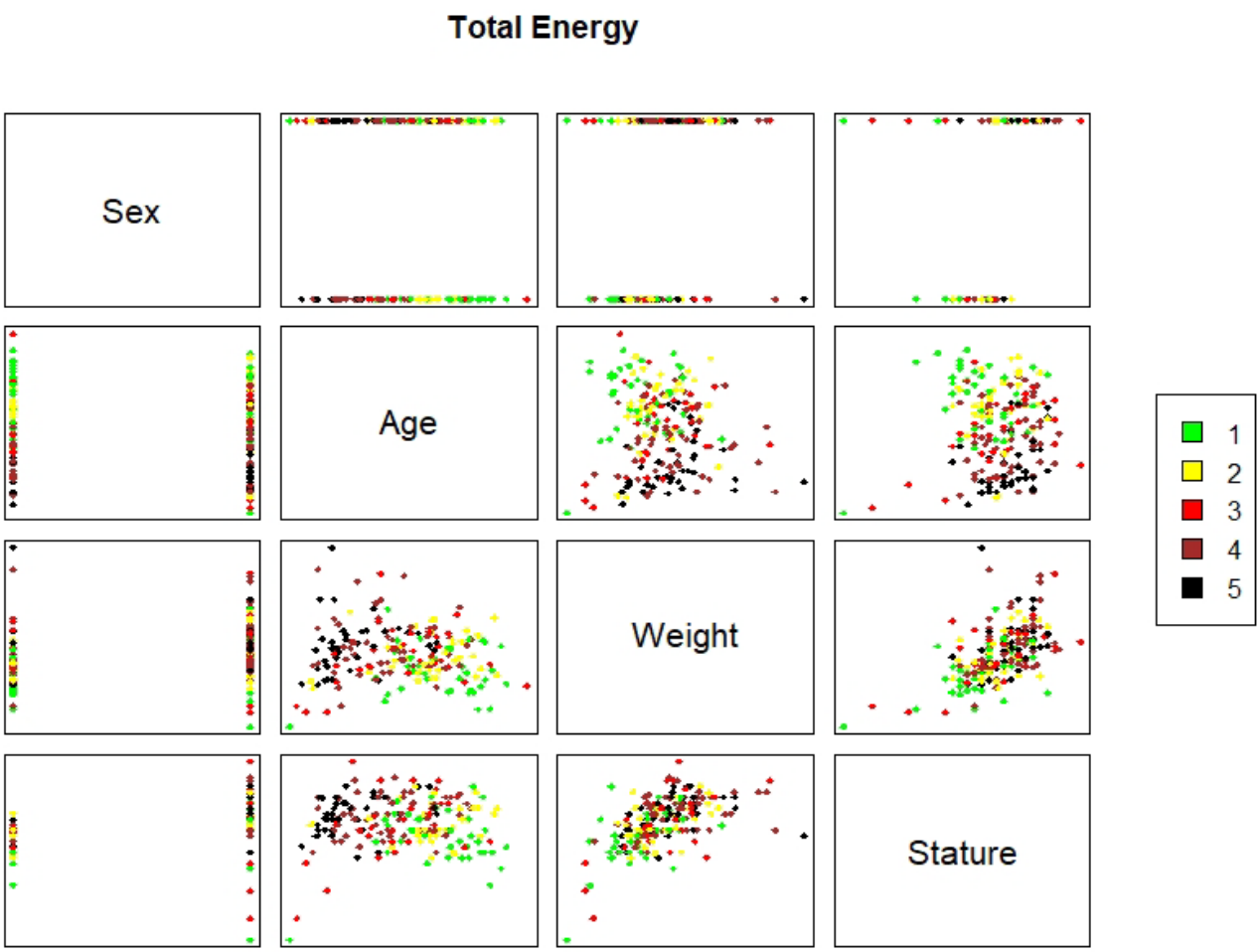

Fig. A5. Exploratory data analysis for all combinations of individual characteristics by vulnerability level (see legend) for total energy. Clustering of light datapoints (vulnerable) versus dark datapoints (less vulnerable) indicates which variables can best distinguish between vulnerability levels. Specific observations to note include: 1) vulnerability is greater at older ages, and 2) clustering is present for interactions of weight and/or stature, notably for vulnerability level 1.